Biophysical Chemistry 24 (1986) 337–356
Elsevier

BPC 01084

VISCOSITY OF CONCENTRATED SOLUTIONS AND OF HUMAN ERYTHROCYTE CYTOPLASM DETERMINED FROM NMR MEASUREMENT OF MOLECULAR CORRELATION TIMES

THE DEPENDENCE OF VISCOSITY ON CELL VOLUME

Zoltán Huba ENDRE** and Philip William KUCHEL *

Department of Biochemistry, University of Sydney, Sydney, NSW 2006, Australia

Received 1st May 1986
Accepted 11th June 1986

Key words: Viscosity; ^{13}C-NMR; Erythrocyte; Longitudinal relaxation time; Correlation time; Cubic closest packing of spheres

Metabolically active human erythrocytes were incubated with [α-^{13}C]glycine which led to the specific enrichment of intracellular glutathione. The cells were then studied using ^{13}C-NMR in which the longitudinal relaxation times (T_1) and nuclear Overhauser enhancements of the free glycine and glutathione were measured. The T_1 values of labelled glycine were also determined in various-concentration solutions of bovine serum albumin and glycerol and also of the natural abundance ^{13}C of glycerol in glycerol solutions. From the T_1 estimates the rotational correlation time (τ_r) was calculated using a formula based on a model of an isotropic spherical rotor or that of a symmetrical ellipsoidal rotor; for glycine the differences in estimates of τ_r obtained using the two models were not significant. From the correlation times and by use of the Stokes-Einstein equations viscosity and translational diffusion coefficients were calculated; thus comment can be made on the likelihood of diffusion control of certain enzyme-catalysed reactions in the erythrocyte. Bulk viscosities of the erythrocyte cytoplasm and the above-mentioned solutions were measured using Ostwald capillary viscometry. Large differences existed between the latter viscosity estimates and those based upon NMR-T_1 measurements. We derived an equation from the theory of the viscosity of concentrated solutions which contains two phenomenological interaction parameters, a 'shape' factor and a 'volume' factor; it was fitted to data relating to the concentration dependence of viscosity measured by both methods. We showed, by using the equation and interaction-parameter estimates for a particular probe molecule in a particular solution, that it was possible to correlate NMR viscosity and bulk viscosity; in other words, given an estimate of the bulk viscosity, it was possible to calculate the NMR 'micro' viscosity or vice versa. However, the values of the interaction parameters depend upon the relative sizes of the probe and solute molecules and must be separately determined for each probe-solute-solvent system. Under various conditions of extracellular osmotic pressure, erythrocytes change volume and thus the viscosity of the intracellular milieu is altered. The volume changes resulted in changes in the T_1 of [α-^{13}C]glycine. Conversely, we showed that alterations in T_1, when appropriately calibrated, could be used for monitoring changes in volume of metabolically active cells.

1. Introduction

Separately, and together, the concentrations of substrates [2] and the intracellular viscosity [3] may influence the rates of metabolic reactions that are necessary for normal cell function. Since erythrocyte shape and rigidity are also influenced by the cell volume and intracellular viscosity, the

* To whom correspondence should be addressed.
** Present address: Department of Biochemistry, University of Oxford, South Parks Road, Oxford OX1 3QU, U.K.

Abbreviations: BSA, bovine serum albumin; Hb, hemoglobin; ϕ, volume fraction; κ, ν, empirical hydrodynamic interaction parameters; η, viscosity; r_o, Stokes radius; τ_r, rotational correlation time; T_1, longitudinal relaxation time; ξ, coefficient of microfriction; $\bar{v}$, partial specific volume.

flow properties of whole blood in the circulation are also influenced directly by the intracellular viscosity [4,5].

Until recently, estimates of intracellular viscosity have been obtained indirectly from viscometry of whole blood [4,5], a technique whose results are highly dependent on the rate of shear; by this experimental means one cannot easily distinguish between the separate contributions of internal viscosity and membrane rigidity. Values of human intraerythrocyte viscosity inferred from torsional viscometry of whole blood are between 2 and 100 mPa s, depending on the rate of shear [4]. Direct measurement of intracellular viscosity in human erythrocytes by using ESR to measure the rotational correlation times (τ_r) of nitroxide spin labels, over the temperature range 18–37°C, have suggested values of 2.5–5.0 mPa s [6–9] *. However, there are significant problems in interpreting these results. Some ESR probes appear to partition into the cell membrane (e.g., Tempone) [6,10]; an unexplained restriction of Tempamine motion has also been reported for Hb-free erythrocyte ghosts [7]. The ESR signal from extracellular nitroxide radicals must be quenched by high concentrations of unphysiological paramagnetic ions such as nickel or ferricyanide [7] and the ESR probes are themselves distinctly 'unphysiological'. A further problem with all of the ESR studies cited is that the spin label τ_r values used to estimate the viscosity of cell cytoplasm have been calibrated against the bulk viscosity of glycerol or sucrose solutions that contained the probe molecules. It is shown in this study that bulk viscosities calculated from probe τ_r values relate only to the solute used for the τ_r measurements.

Measurements of τ_r and of coefficients of translational diffusion of intracellular water protons in intact animal and plant cells by NMR indicate that the intracellular viscosity is only about twice that of pure water at the corresponding temperature [11]. However, water proton τ_r values in intact cells and protein solutions are dominated by a small fraction of 'bound' water (with short relaxation times) which exchanges rapidly with molecules of bulk water, the latter having τ_r values close to those of pure water [11]. Furthermore, the interpretation of intracellular viscosity estimates based on the restriction to motion of water molecules is controversial in view of the debate over the amount of 'vicinal' water in intact cells and also the question of accessibility of all cell water to ions and small molecules [12].

A simpler NMR method used for probing intracellular viscosity in suspensions of human erythrocytes at 37°C involves measuring the ^{13}C longitudinal relaxation times (T_1) of ^{13}C-labelled physiological intracellular molecules; we used glycine and glutathione (GSH) [3]. The method relies on the facilitated diffusion of [α-^{13}C]glycine into erythrocytes during incubation at 37°C and on the subsequent enzyme-catalysed incorporation of the labelled glycine into intracellular GSH [13]. This NMR method yields intracellular viscosity estimates which are approximately twice that of pure water, i.e., approx. 1.4 mPa s at 37°C [3].

In the present work we explain why the ^{13}C-NMR estimates of intraerythrocyte viscosity are significantly lower than those obtained using ESR despite both methods depending on the observation of the τ_r of a small intracellular probe molecule. The dependence of the intracellular NMR viscosity on cell volume was also examined in order to determine the maximum range of intracellular viscosities attainable physiologically and thus to assess the potential effect of changing cell volume on the rates of diffusion-controlled enzyme reactions in human erythrocytes.

NMR-glycine-viscosity estimates were obtained using τ_r values calculated from ^{13}C-NMR measurement at 37°C of T_1 of a constant low concentration of [α-^{13}C]glycine in BSA and glycerol solutions and also in intact human erythrocytes. The estimates were compared with those of the bulk viscosity, obtained by capillary viscometry.

Different values of the NMR-based viscosity measurements, with glycine as the probe molecule, were obtained for glycerol and BSA solutions that had the same bulk viscosity; the results indicated that the relative size of probe and solute molecules affected the estimate of viscosity. A simple geo-

* Absolute viscosity values were calculated from published relative viscosity values by multiplying by the absolute viscosity of pure water [1], at the temperature of the experiment.

metrical model is proposed to describe the different extent of hydrodynamic interaction that occurs between a particular probe molecule and different solute molecules.

By application of a mathematical treatment of the viscosity of concentrated solutions, values of phenomenological hydrodynamic interaction parameters were determined; these allowed the viscosity dependence of NMR-derived τ_r values to be predicted. This analysis also enabled the bulk viscosity to be calculated from the NMR viscosity and vice versa; consequently, it was possible to calculate the bulk viscosity in intact erythrocytes over a range of cell volumes.

Finally, we demonstrated that changes in the volume of actively metabolizing erythrocytes may be monitored using the viscosity calculated from the estimate of T_1 of a suitably labelled probe molecule.

2. Materials and methods

2.1. Materials

BSA (powder, fraction V) was obtained from Sigma, St. Louis, MO, [α-^{13}C]glycine from Merck, Sharp and Dohme, Pointe Claire Dorval, Quebec, and glycerol (> 99% pure) from British Drug Houses, Poole, Dorset. Carbogen ($O_2 : CO_2 = 19 : 1$) was from Commonwealth Industrial Gases, Alexandria, NSW, Australia and ^2H_2O (99.75%) was from the Australian Institute of Nuclear Science and Engineering, Lucas Heights, NSW. All other chemicals were of AR grade. NMR tubes were from Wilmad, Buena, NJ.

2.2. Erythrocyte preparation

Freshly drawn, washed human erythrocytes were gassed with Carbogen for 10 min at 25°C, then incubated in glucose-free isotonic phosphate buffer at 37°C with [α-^{13}C]glycine (25 mmol/l) for approx. 4 h; this was sufficiently long to allow influx of the [α-^{13}C]glycine and labelling of approx. 50% of GSH [3]. The exchange between free glycine and the glycyl of GSH was then inhibited by washing the cells twice in Krebs-bicarbonate buffer in ^2H_2O containing glucose (10 mmol/l). The cells were then washed three times with five volumes of solutions of NaCl in ^2H_2O at 4°C; these had osmolalities measured at 37°C [3] of 215, 300 or 577 mosmol/kg. These suspensions were reoxygenated with Carbogen and sampled for erythrocyte count and hematocrit [14]. The hematocrit was adjusted to ≥ 0.95 and 1.8 ml of each suspension was dispensed into 10-mm NMR tubes. The samples were stored at 4°C until just prior to NMR measurement, when they were warmed to 37°C.

2.3. Solution preparation

Stock BSA solutions were prepared by adding 5 g to 10 ml ^2H_2O followed by slow intermittent agitation with a magnetic stirrer under vacuum at room temperature. The osmotic pressure of the solution was measured (140 mosmol/kg) and then increased by direct addition of NaCl and [α-^{13}C]glycine to 5 ml of the solution, giving a final osmolality of 290 mosmol/kg and a glycine concentration of 10 mmol/l. After ^{13}C-NMR T_1 measurements had been undertaken the bulk viscosity of the solutions was measured at 37°C. The pD ($\equiv$ p^{2}H, uncorrected pH reading) of these solutions ranged from 6.22 ([BSA] = 0 g/dl) to 7.16 ([BSA] = 50 g/dl).

Glycerol solutions were prepared by dilution with isotonic saline/^2H_2O. A constant volume of [α-^{13}C]glycine in ^2H_2O, 0.3 M, was added to 4 ml of each dilution, giving a final glycine concentration of 10 mmol/l. Solution density was calculated from the glycerol density and that of ^2H_2O (1.1052 g/ml at 20°C [1]). The bulk viscosity of each solution was measured at 37°C. The pD of these solutions ranged from 6.22 ([glycerol] = 0 g/100 g) to 7.14 ([glycerol] = 82 g/100 g). Prior to ^{13}C-NMR T_1 measurement 1–2 mg EDTA was added directly to each (1.8 ml) NMR sample to bind paramagnetic impurities.

2.4. ^{13}C-NMR measurements

T_1 and nuclear Overhauser enhancement (NOE) measurements were made at 37°C using a Bruker WM400 spectrometer operated in the pulsed

Fourier transform mode; the spectrometer frequency for ^{13}C was 100.62 MHz. The main details of the pulse sequences have been reported [3]; but here we used two-level, gated, broadband proton decoupling with switching from low to high power during data acquisition. Sample temperature was checked for radiofrequency-induced heating by using a thermocouple; none occurred. There was good agreement between estimates of intracellular viscosity measured from glycine and GSH T_1 values. Therefore, the more time-consuming GSH-glycyl measurements were performed on only one sample (osmolality 215 mosmol/kg). A total of 64 transients for GSH-glycyl and 16 transients per spectrum for glycine were averaged for each of the T_1 and NOE measurements in intact cells; for the measurements on [α-^{13}C]glycine in BSA and glycerol solutions, 16 transients were averaged. Natural abundance ^{13}C T_1 measurements on glycerol were also obtained from the glycerol solutions by averaging 16 transients per spectrum. A spectral width of 16 kHz was used in all experiments. The T_1 values were determined from a three-parameter exponential fit onto each data set by non-linear least-squares analysis [15].

2.5. Rotational correlation times

Estimates of τ_r were obtained from T_1 values by iterative refinement of an initial value using an expression for T_1 incorporating the appropriate spectral density function [16,17]. Spectral density functions relating to spherical and symmetrical ellipsoidal rotors were used to calculate each τ_R of [α-^{13}C]glycine from the T_1 value.

3. Theory

3.1. Concentration dependence of viscosity

The dependence of bulk viscosity on a wide concentration range of solutes is described by several different expressions; for suspensions of spheres (volume fraction ϕ) the relative viscosity ($\eta_R = \eta/\eta_0$, η_0 being the viscosity of pure solvent) has variously been given by: $\eta_R = (1 - 1.35\phi)^{-2.5}$ [62,63]; $\eta_R = 1.82\phi^2/(1 - 1.35\phi)^3$ for large ϕ [64]; $1 + 2.5\phi + 2.635\phi^2 + \ldots\ldots$ for low values of ϕ [64] and for extremely dilute solutions (suspensions), $\eta_R = 1 + 2.5\phi$ [19,20]. However, the most useful functional form for the present work is that of Mooney [18];

$$\eta_R = \exp[2.5\phi/(1 - \kappa\phi)], \tag{1}$$

where κ is a molecular 'interaction' parameter which accounts for first-order hydrodynamic interactions. For a suspension consisting of spheres of two markedly different diameters, eq. 1 becomes:

$$\eta_R = \exp[2.5\phi_1/(1 - \kappa\phi_1 - \phi_2)] \times \exp[2.5\phi_2/(1 - \kappa\phi_2)]. \tag{2}$$

where ϕ_1 and ϕ_2 are the volume fractions of spheres with smaller and larger radii, respectively [18]. The factor 2.5 was chosen so that in the limit of $\phi \to 0$ eq. 1 yields the expression developed by Einstein [19,20]; the latter applies only to very dilute solutions of spherical molecules in which no long range hydrodynamic interactions occur between the molecules, viz:

$$\eta_R = 1 + 2.5\phi. \tag{3}$$

However, there is little justification for using the value 2.5 for concentrated solutions; consequently, we replaced 2.5 by an arbitrary 'shape' factor, ν, so that eq. 1 becomes:

$$\eta_R = \exp[\nu\phi/(1 - \kappa\phi)], \tag{4}$$

and in the present work the values of both ν and κ were determined experimentally by non-linear least-squares regression of eq. 4 onto viscosity versus solute-concentration data obtained using both NMR T_1 estimates and capillary viscometry. The volume fraction of solute in each sample was calculated from $\phi = c\bar{v}$, where c is the solute concentration (g/ml) and $\bar{v}$ the partial specific volume (ml/g). Values of $\bar{v}$ used were 0.7360 ml/g for BSA and 0.7546 ml/g for Hb [21]. A value of 0.4617 ml/g was calculated for glycerol by assuming the molecules to be spherical with the same packing density as liquid water molecules (0.58 [22]); while this value may be an underestimate, the general conclusions reached here were independent of a precise value (see section 5). The

average volume of glycine residues in a protein crystal is 66.4 Å^3 [23]. Thus, $\bar{v}$ of glycine is 0.6218 ml/g and the volume fraction occupied by 10 mmol/l glycine is 4.7×10^{-4} l/l solution.

3.2. NMR viscosity (η_N) as a function of the bulk viscosity (η_B)

Following the separate determinations of η_N and η_B on the same samples it was possible to calculate values of the interaction parameters, ν and κ from a range of solute concentrations studied by the two methods. The interrelationship of η_N and η_B is derived from eq. A4 (appendix A) and is given by:

$$\eta_N = (\eta_B)^{\psi}, \tag{5}$$

where

$$\psi = \nu_N / \{\nu_B + \ln(\eta_B)[\kappa_B - \kappa_N]\} \tag{6}$$

and

$$\eta_B = (\eta_N)^{\psi^*}, \tag{7}$$

where

$$\psi^* = \nu_B / \{\nu_N + \ln(\eta_N)[\kappa_N - \kappa_B]\}. \tag{8}$$

Thus, given estimates of η_N and η_B for a particular solution and probe molecule, eqs. 7 and 8 allow intracellular bulk viscosity to be calculated from measurements of η_N in intact cells.

3.3. Rotational correlation time (τ_r) and viscosity

For an isotropic spherical rotor the relationship between τ_r and viscosity is given by [24]:

$$\tau_r = 4\pi\eta r_o^3 / 3kT, \tag{9}$$

where r_o is the Stokes radius, k the Boltzmann constant and T the absolute temperature. It is normally assumed that η represents the bulk viscosity of the solution. For solutions in which the solvent molecules have finite dimensions with respect to those of the solute molecules, the Stokes expression for rotational friction ($8\pi\eta r_o^3$) is multiplied by a coefficient of microfriction, ξ, given by:

$$\xi = \left[6r_s/r_o + 1/(1 + r_s/r_o)\right]^{1} \tag{10}$$

where r_s is the radius of the spherical solvent molecules [25]. An equivalent factor to ξ has not been calculated for symmetrical ellipsoids but ξ may provide a reasonable approximation [26].

For a tumbling symmetrical ellipsoid of revolution there are two independent correlation times, $\tau_\perp$ for motion perpendicular to, and $\tau_\parallel$ for motion parallel to, the axis of symmetry. These are functions of solution viscosity according to:

$$\tau_\perp = \left[32\pi a^3 S'/18kT\right]\eta = K'\eta, \tag{11}$$

and

$$\tau_\parallel = \tau S''/S', \tag{12}$$

where a and b are the respective lengths of the semimajor and semiminor axes, K', S' and S'' are constants and where, for prolate ellipsoids ($a > b$),

$$S' = (1 - q^4)/\left[(2 - q^2)aS - 2\right], \tag{13}$$

$$S'' = q^2(1 - q^2)/(2 - q^2 aS), \tag{14}$$

$$S = 2\ln\left\{\left[a + (a^2 - b^2)^{0.5}\right]/b\right\}/(a^2 - b^2)^{0.5}, \tag{15}$$

and $q = b/a$ [16]. Thus, for both isotropic and anisotropic motion, the correlation times are linear functions of viscosity in an ideal solution.

In the present work the microfriction coefficient, ξ, was not included since the Stokes radius, r_o, and the ellipsoidal shape parameters, a^3S' and a^3S'', were determined experimentally from the measured value of T_1 (and hence τ_r) and of the bulk viscosity (η_B) for the most dilute BSA and glycerol solutions by substitutions of the experimental estimates of these latter parameters into eq. 9, 11 or 12. The values of r_o, a^3S' and a^3S'' may be regarded simply as constant experimental geometrical parameters. ξ represents the factor by which the Stokes coefficient must be multiplied in order to obtain the true (experimental) frictional coefficient [25]. Consequently, comparison of values of either τ_r, rotational diffusion coefficients, or of η_N obtained using the experimental geometrical parameters, with those estimates obtained using geometrical parameters determined by X-ray crystallography provides a novel way of estimating ξ. Once the geometrical parameters were estimated

in the most dilute solution, NMR viscosity estimates in the other solutions were calculated from the τ_r values using either:

$$\eta_N = \tau_r 3kT/4\pi r_o^3, \tag{16}$$

or

$$\eta_N = \tau/K'. \tag{17}$$

This assumes that molecular size and shape do not change with concentration. At least theoretically, changes in solvation and aggregation are concentration-dependent [27], but in the case of Hb only very small changes in solvation have been reported with varying solute concentration [21].

Two further simplifications are possible. First, it is not necessary to determine both $\tau_\perp$ and $\tau_\parallel$ for a symmetrical ellipsoid, since the two correlation times are related through the ellipsoid geometry [16] (see eq. 12). Secondly, when the geometrical factors are determined experimentally in the most dilute solution K' is equal to $3kT/4\pi r_o^3$; consequently eqs. 16 and 17 will be identical. Thus, identical values of η_N are obtained from the experimental measurements of T_1 of a probe in dilute solution whether an isotropic spherical rotor or an anisotropic symmetrical-ellipsoidal-rotor model is used. The former method is simpler and was therefore preferred for the studies reported here.

An alternative approach for estimating η_N is to use the inverse relationship between T_1 and viscosity which exists under conditions of low viscosity when the extreme motional narrowing limit prevails, i.e., $(\omega_H + \omega_C) \ll 1/\tau_r$ [24]. If T_0 is the value of T_1 for a probe molecule in a solution of known viscosity η_0, then for a solution of unknown viscosity (η_N, T_X):

$$\eta_N = \eta_0 T_0/T_X. \tag{18}$$

Such an approach has been used previously [28] and we show here that both T_1-ratio and correlation-time methods yield identical results except that the error associated with the τ_r method is significantly greater since an error in r_o to the third power must be considered. An estimate of r_o is required in order to calculate the translational diffusion coefficient (D_T) from η_N using the Stokes-Einstein equation [29–31]:

$$D_T = kT/6\pi\eta r_o. \tag{19}$$

As in the case of determining τ_r, the use of an experimentally determined value of r_o in eq. 19 corrects D_T for the coefficient of microfriction.

For concentrated solutions eq. 9 must be modified since it was derived originally by assuming that no interaction takes place between the solute molecules [32,33]. By incorporating eq. 1, an adequate phenomenological description of the viscosity dependency of correlation time is given by:

$$\tau_r = \left(4\pi r_o^3/3kT\right)\eta_N, \tag{20}$$

where η_N is determined from η_B using eqs. 5 and 6.

3.4. *Erythrocyte volume as a function of NMR viscosity*

As derived in appendix B, it is possible to describe cell volume (V) in terms of η_N using:

$$V = V_{ISO}\left\{F + \bar{v}Hb_{ISO}(1-F)\left[\nu_N/\ln(\eta_N) + \kappa_N\right]\right\} \tag{21}$$

where V_{ISO} is the volume of normovolemic erythrocytes (at isotonicity), Hb_{ISO} the concentration of Hb in normovolemic cells, F the volume fraction (relative to V_{ISO}) occupied by cell membranes and non-Hb protein (i.e., $F \equiv 1 -$ volume fraction of cell water $- \phi_{Hb}$) and $\bar{v}$ the partial specific volume of Hb. The intracellular concentration of Hb(Hb_{IC}) at any given cell volume was calculated from:

$$Hb_{IC} = Hb\left[V_{ISO}/(V - FV_{ISO})\right], \tag{22}$$

where Hb is g(Hb)/(ml packed isovolemic cells); this definition averages Hb_{IC} over the total intracellular volume including the volume occupied by Hb itself. The values of the parameters used were: Hb 0.335 g/ml [34]; V_{ISO} 80.7 fl; Hb_{ISO} 0.3515 g/ml; and F 0.047 (assuming that the intracellular water occupies 0.7 of the total cell volume; [35]). ν_N and κ_N were obtained experimentally for intracellular glycine (see below).

3.5. Bulk viscosity (η_B) measurements

Measurements of η_B were obtained using an Ostwald (capillary) viscometer in a water bath thermostatically controlled by a mercury regulator (Townson & Mercer, Croydon, Surrey); the temperature was equilibrated at 37 ± 0.01°C. The same viscometer was used for all measurements and was mounted so that it always occupied precisely the same position in the bath. Flow times were recorded to within 0.01 s. Solutions were temperature equilibrated and passed once through the capillary before any measurements were made. From four to eight flow-time measurements were made on each solution.

The relative viscosity of a solution (X) was determined from:

$$\eta_R = (\rho_X/\rho_0)(t_X/t_0) \tag{23}$$

where ρ is the solution density, t the flow time and subscript 0 refers to the water reference solution [36]. Solution density was calculated from [36]:

$$\rho_X = \rho_0\left[1 - c\bar{v}/100 + c/(100\rho_0)\right], \tag{24}$$

where c is the concentration (g/dl) and $\bar{v}$ the partial specific volume of the solute. The absolute viscosity was then calculated by multiplying η_R by η_0, where $\eta_0(H_2O) = 0.6915$ at 37°C [1].

Where normalised values of η_B or η_N were used these were obtained by dividing the absolute value by the measured bulk viscosity of isotonic saline at 37°C (0.76 mPa s).

3.5. Computing and statistical analyses

Non-linear least-squares analyses were performed on Cyber 720 and 825 computers using the modified Levenberg-Morrison-Marquardt algorithm [37]. Graphs were plotted using a Tektronix 4052 graphics computer.

Weighted means (X_M) were calculated from:

$$X_M = \sum(w_i x_i)/\sum w_i \tag{25}$$

where w_i is the weight of the i-th mean and the x_i are independent: $w_i = 1/\text{S.D.}^2$ (S.D., standard deviation) was used in all cases.

Standard deviations of the parameters T_1, ν and κ were estimated in the course of the non-linear least-squares regression of the relevant equation onto the respective basic data. However, error estimates of parameter values derived from these three parameters were calculated using the general formula for the variance (var) of a function of several variables:

$$\text{var}[g(x)] = \sum\left[g_i'(\theta)\right]^2 \text{var}(x_i) + \sum\sum\left[g_i'(\theta_i)g_i'(\theta_j)\,\text{cov}(x_i, x_j)\right], \tag{26}$$

where $g(x) = g(x_1, x_2, \ldots, x_k)$ and $g_i'(\theta) = \partial[g(x)]/\partial x_i$ are evaluated at $\theta_1, \theta_2, \ldots, \theta_k$ [38].

Since estimates of all the variables used were obtained by independent measurement, $\text{cov}(x_i, x_j) = 0$ and S.D. were obtained from $\sqrt{\text{var}}$. The following specific applications of this analysis were used frequently. $E[g(x)]$ represents the estimate of the mean value of $g(x)$, i.e., the expectation value of $g(x)$, and CV the coefficient of variation of the parameter.

Viscosity

(A) Correlation time method

$$\text{var}(\eta) = E^2(\eta)\left[CV^2(\tau_r) + 9CV^2(r_0)\right]. \tag{27}$$

(B) T_1 ratio method

$$\text{var}(\eta) = E^2(\eta)\left[CV^2(\eta_0) + CV^2(T_0) + CV^2(T_X)\right]. \tag{28}$$

Translational diffusion

$$\text{var}(D_T) = E^2(D_T)\left[CV^2(\eta) + CV^2(\tau_r)\right]. \tag{29}$$

Stokes radius

$$\text{var}(r_0) = E^2(r_0)\left[CV^2(\eta) + CV^2(\tau_r)\right]. \tag{30}$$

Rotational correlation time

At the extreme narrowing limit:

$$\text{var}(\tau_r) = E^2(\tau_r)CV(T_1). \tag{31}$$

Weighted mean

$$\text{var}(X_M) = 1/\sum w_i. \tag{32}$$

3.6. Intermolecular separation as a function of concentration

As derived in appendix C for the particular case of intracellular Hb, the edge-to-edge separation (dm) can be estimated from:

$$\text{Separation} = 2[M/N_A]\{[1/2c]^{1/3}/\sqrt{2} - [3\bar{v}/4\pi]^{1/3}\} \quad (33)$$

where M is the molecular weight, c the concentration (g/ml), and N_A Avogadro's number.

4. Results

4.1. η_N and η_B in BSA and glycerol solutions

Estimates of the bulk viscosity (η_B) and T_1, as well as data derived from these measurements [spherical rotor correlation times and viscosities calculated from T_1 by both T_1-ratio (η-N1) and correlation-time (η-N2) methods], are given in tables 1–3. The Stokes radius of glycine, r_o, was taken as the weighted mean of four estimates; it was calculated using eq. 9 and the measured bulk viscosity, and τ_r of 10 mM [α-^{13}C]glycine, in isotonic saline.

These data illustrate that T_1, τ_r and viscosity are all solute-concentration dependent. However, with increasing concentration, the increase in NMR viscosity was less than that observed for the bulk viscosity. T_1-ratio and correlation-time methods yield similar viscosity estimates (identical, if a single estimate of the Stokes radius was used in the calculation of η-N2). As anticipated, larger standard deviations were calculated for the estimates obtained for the correlation-time method. The data for bulk viscosity and NMR viscosity (η-N2 only) are compared in figs. 1 and 2. The results illustrate that, with increasing solute concentration, the increase in NMR-glycine-viscosity was less than the observed increase in η_B. The difference between the estimates was less when the viscosity was adjusted with glycerol (fig. 2) than when BSA was used (fig. 1). Nevertheless, a progressively increasing difference remained, even when a self-probe, natural abundance ^{13}C-labelled glycerol, was used instead of [α-^{13}C]glycine to probe the viscosity of the glycerol-water solutions (fig. 2). The values of the ν and κ determined by non-linear regression of eq. 4 onto the normalised viscosity data are given in the legend of each figure; these parameters were then used to draw the solid lines through each data set. Eq. 2 was also fitted to each data set by using a value of 4.7×10^{-4} for ϕ(glycine) and substituting ν for the factor 2.5. However, because the volume oc-

Table 1

The concentration dependence of T_1, correlation time and viscosity

Viscosity adjusted with BSA, NMR probe: [α-^{13}C]glycine. Temperature, 37°C. Each solution contained [α-^{13}C]glycine (10 mmol/l). The same solutions were used for both viscometry and NMR relaxation measurements. τ_r was calculated assuming isotropic motion of a spherical rotor. Viscosity measurements were calculated from Ostwald viscometry (η_B), the T_1 ratio (eq. 18; η-N1) and τ_r (eq. 16; η-N2). The Stokes radius of glycine used to calculate η-N2 was 1.7400 ± 0.008 (the weighted mean of four separate estimations made under identical conditions). Error estimates represent 1 standard deviation (S.D.). The S.D. of τ_r may be obtained by using eq. 31 to calculate the variance. NOE measurements were not significantly different from 2.988.

[BSA] (g/dl)	T_1 (s)	τ_r (s)($\times 10^{12}$)	η_B (mPa s)	η-N1 (mPa s)	η-N2 (mPa s)
0.000	5.99 ± 0.33	3.89	0.759 ± 0.003	0.759 ± 0.005	0.76 ± 0.04
3.125	6.05 ± 0.33	3.85	0.832 ± 0.005	0.751 ± 0.005	0.75 ± 0.04
6.25	4.70 ± 0.31	4.95	0.920 ± 0.004	0.967 ± 0.007	0.96 ± 0.07
9.375	4.18 ± 0.29	5.57	1.013 ± 0.007	1.088 ± 0.009	1.08 ± 0.08
12.5	4.13 ± 0.12	5.64	1.136 ± 0.005	1.101 ± 0.004	1.09 ± 0.04
15.625	4.11 ± 0.25	5.66	1.294 ± 0.010	1.106 ± 0.007	1.10 ± 0.07
30.0	3.07 ± 0.19	7.58	2.91 ± 0.04	1.481 ± 0.010	1.47 ± 0.10
50.0	2.47 ± 0.14	9.43	31.7 ± 2.4	1.841 ± 0.012	1.83 ± 0.11

Table 2

The concentration dependence of T_1 relaxation, correlation time and viscosity

Viscosity adjusted with glycerol. NMR probe: [α-^{13}C]glycine. Temperature, 37°C. Details are as for table 1. No NOE measurement was significantly different from 2.988. The variation in T_1 errors represents fluctuations in instrument performance within a continuous sequence of experiments.

[Glycerol] (g/100 g)	T_1 (s)	τ_r (s)($\times 10^{12}$)	η_B (mPa s)	η-N1 (mPa s)	η-N2 (mPa s)
0	5.9 ±0.6	3.95	0.8495 ± 0.0010	0.850 ± 0.021	0.76 ± 0.08
6	6.5 ±0.9	3.58	0.9583 ± 0.0018	0.771 ± 0.023	0.69 ± 0.10
11	4.2 ±0.5	5.54	1.1033 ± 0.0013	1.193 ± 0.025	1.07 ± 0.13
22	2.9 ±0.7	8.03	1.473 ± 0.003	1.73 ± 0.12	1.6 ± 0.4
35	2.39 ±0.08	9.74	2.2213 ± 0.0029	2.097 ± 0.011	1.89 ± 0.07
38	2.44 ±0.09	9.54	2.4355 ± 0.0010	2.054 ± 0.012	1.85 ± 0.07
60	1.35 ± 0.06	17.27	6.0585 ± 0.0024	3.713 ± 0.012	3.34 ± 0.15
82	0.337 ± 0.009	71.24	33.71 ±0.05	14.87 ±0.16	13.8 ±0.4

cupied by glycine molecules is insignificant compared with that occupied by the main solute(s), there was no difference in the values of ν or κ obtained.

4.2. τ_r as a function of η_B

The progressive deviation of experimentally determined values of τ_r from those predicted by eq. 9 for an 'ideal' solution is illustrated in figs. 3 and 4. As anticipated from the results shown in figs. 1 and 2, τ_r(glycine) is more sensitive to changes in η_B induced by glycerol than to changes of equal magnitude induced by BSA. The lines drawn through the experimental τ_r values in figs. 3 and 4 were calculated using eq. 20, with η_N values determined from η_B using eqs. 5 and 6.

4.3. NMR-glycine-viscosity in Hb solutions and in intact cells

The measurement of T_1 and NOE for intracellular [α-^{13}C]glycine is illustrated in figs. 5 and 6. T_1 and NOE values and derived hydrodynamic parameters for [α-^{13}C]glycine in human erythrocytes at three representative cell volumes are sum-

Table 3

The concentration dependence of T_1 relaxation, correlation time and viscosity

Viscosity adjusted with glycerol. NMR probes: glycerol [-^{13}CH-] and glycerol [-^{13}CH$_2$] [a]. Temperature 37°C.

[Glycerol] (g/100 g)	[-CH-] T_1 (s)	[-CH$_2$] T_1 [b] (s)	[-CH-] τ_r (s)($\times 10^{12}$)	[-CH$_2$] τ_r (s)($\times 10^{12}$)	η_B (mPa s)	[-CH-] η-N2 (mPa s)	[-CH$_2$] η-N2 (mPa s)
6	6.2 ±0.6	3.8 ±0.4	7.51	6.13	0.9583 ± 0.0018	0.96 ± 0.13	0.96 ± 0.15
11	4.1 ±0.5	2.3 ±0.3	11.36	10.13	1.1033 ± 0.0013	1.45 ± 0.22	1.58 ± 0.27
22	4.6 ±0.4	2.25 ±0.05	10.13	10.35	1.473 ±0.003	1.29 ± 0.16	1.62 ± 0.19
35	2.9 ±0.3	1.61 ±0.24	16.08	14.47	2.2213 ± 0.0029	2.05 ± 0.28	2.26 ± 0.25
38	2.8 ±0.4	1.71 ±0.12	16.65	13.63	2.4355 ± 0.0010	2.13 ± 0.36	2.13 ± 0.28
60	1.75 ± 0.25	0.999 ± 0.019	26.72	23.38	6.0585 ± 0.0024	3.4 ±0.6	3.65 ± 0.42
80	0.60 ± 0.02	0.37 ±0.01	80.75	64.55	33.71 ±0.05	10.3 ±1.0	10.1 ±1.2

[a] Natural abundance ^{13}C. Other details as for table 1. Note that η-N2 measurements were calculated from τ_r.

[b] The samples were identical to those used in table 2; both glycerol relaxation and bulk viscosity data were derived from the same experiments as the data for glycine in table 2. The increase in self-concentration of the glycerol probe has not been considered in the calculation of η-N2.

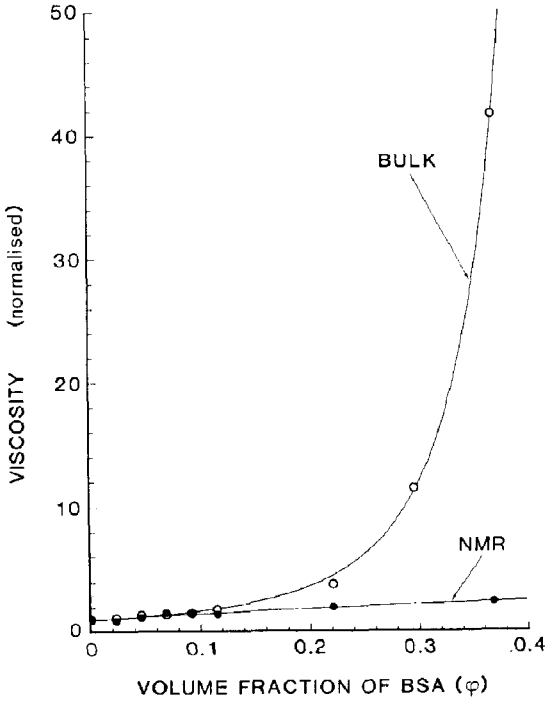

Fig. 1. NMR and bulk viscosity versus volume fraction of BSA; the viscosity was adjusted with BSA and the NMR probe was [α-^{13}C]glycine. Temperature 37°C. (●) NMR data, (○) bulk viscosity measurements. The lines were calculated by non-linear least-squares regression of eq. 4 onto the data. The interaction parameters obtained were: NMR viscosity, $\nu = 5.1 \pm 0.6$, $\kappa = -2.99 \pm 0.8$ bulk viscosity, $\nu = 4.61 \pm 0.14$, $\kappa = 1.48 \pm 0.04$. Viscosity measurements were normalised so that $\phi = 0$, $\eta = 1$.

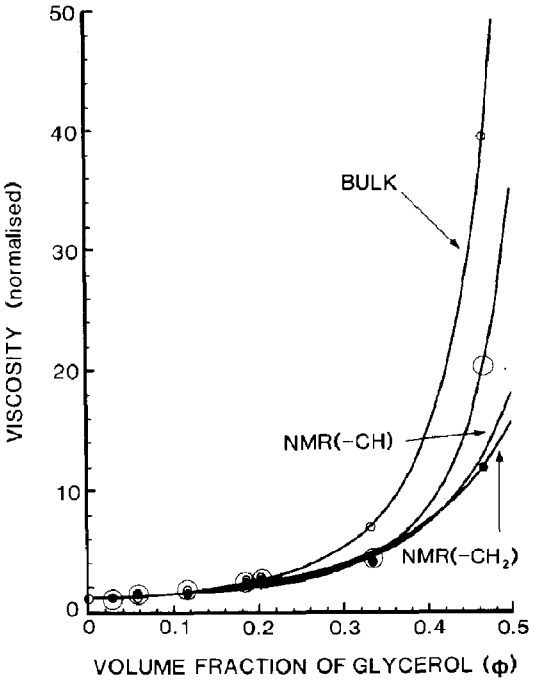

Fig. 2. NMR and bulk viscosity versus volume fraction of glycerol; the viscosity was adjusted with glycerol and the temperature was 37°C. The interaction parameters calculated for the bulk viscosity (○) were $\nu = 3.68 \pm 0.07$, $\kappa = 1.146 \pm 0.020$ and for the NMR-[α-^{13}C]glycine-viscosity (○) $\nu = 2.76 \pm 0.28$, $\kappa = 1.23 \pm 0.09$. NMR viscosity calculated from natural abundance glycerol [-^{13}CH-] and glycerol [-^{13}CH$_2$] (●) NMR-CH-viscosity, $\nu_{N1} = 3.1 \pm 0.3$, $\kappa_{N1} = 0.91 \pm 0.14$; NMR-CH$_2$-viscosity, $\nu_{N2} = 3.6 \pm 0.4$, $\kappa_{N2} = 0.70 \pm 0.18$. Although the individual data points for NMR viscosity determined by each glycerol probe were indistinguishable graphically, the interaction parameters obtained by non-linear regression analysis differed sufficiently to yield the separate lines shown.

marised in table 4. The data illustrate the progressive decrease in T_1 and increase in η_N with decreasing cell volume. Also shown are the data obtained in swollen erythrocytes (volume 115.8 fl) using [*glycyl*-α-^{13}C]GSH as the viscosity probe. As anticipated from previous studies in normovolemic erythrocytes [3], in spite of large differences between glycine and GSH-glycyl T_1, and hence τ_r, values, reasonably (see section 5) similar values for intracellular η_N were obtained with each probe.

The intracellular Hb concentration (and hence ϕ_{Hb}) at each of these cell volumes was calculated by using eq. 22. Therefore, it was possible to use the η_N data at each volume to calculate the interaction parameters, ν_N and κ_N, for the intracellular Hb solution probed by [α-^{13}C]glycine in the same way that these parameters were obtained in BSA and glycerol solutions. Bulk viscosity interaction parameters, ν_B and κ_B, were determined by a non-linear least-squares fit of eq. 4 onto published data for Hb [39]. The results are shown in table 2. Also shown are normalised values of intracellular η_B calculated from η_N of the intact erythrocytes by using eqs. 7 and 8; these may be converted to absolute values at 37°C by multiplying by η_0 (0.76 mPa s; table 1). The experimental intracellular η_B is shown in fig. 7. This illustrates that the

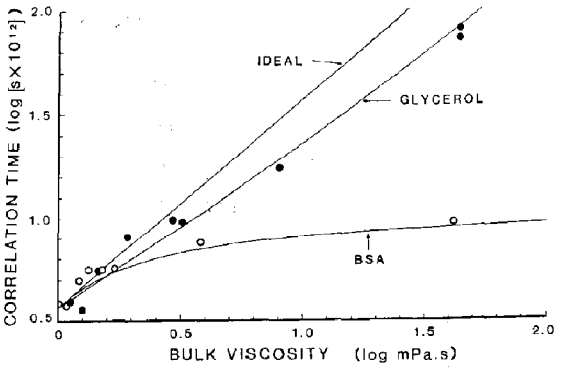

Fig. 3. [α-^{13}C]Glycine correlation time as a function of normalised bulk viscosity. Temperature 37°C. (○) Viscosity adjusted with BSA; (●) viscosity adjusted with glycerol. The line marked 'ideal' is a plot of $\tau_r = 4\pi\eta r_o^3/3kT$ with r_o (1.583 × 10^{-8} cm) determined from the solution of lowest (normalised) viscosity. The log-log plot was used for compression of the axes. Data are from tables 1 and 2. Eq. 20 was fitted to the empirical data using the interaction parameters listed in the legends to figs. 1 and 2.

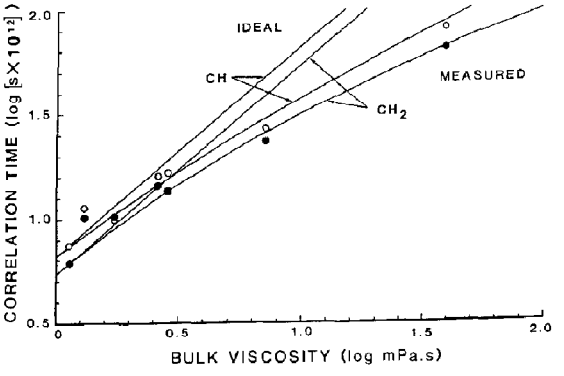

Fig. 4. Glycerol correlation time as a function of normalised bulk viscosity. Temperature 37°C. Viscosity was adjusted with glycerol. (○) Glycerol [-^{13}CH-]; (●) glycerol [-$^{13}CH_2$]. The solid lines are plotted as for fig. 3 with the Stokes radius calculated as 1.895×10^{-8} cm for [-^{13}CH] and 1.770×10^{-8} cm for [-$^{13}CH_2$]. Data were derived from tables 2 and 3. Other details as for fig. 3.

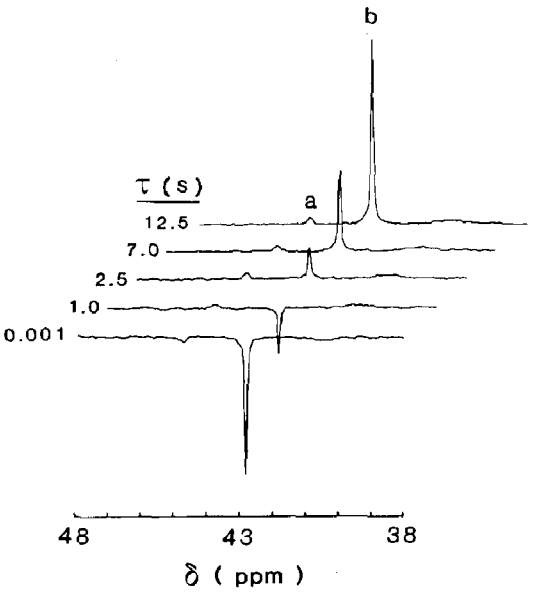

Fig. 5. Measurement of T_1 of predominantly intracellular [α-^{13}C]glycine (b) in human erythrocytes (in isotonic Krebs buffer; *Hc*, 0.80) by the inversion-recovery method. Spectra of partially relaxed spins at five different delay times between the 180 and 90° pulses. NMR: 16 transients per spectrum; 37°C. Peak a is [*glycyl*-α-^{13}C]GSH. Selective proton decoupling of ^{13}C at resonance b.

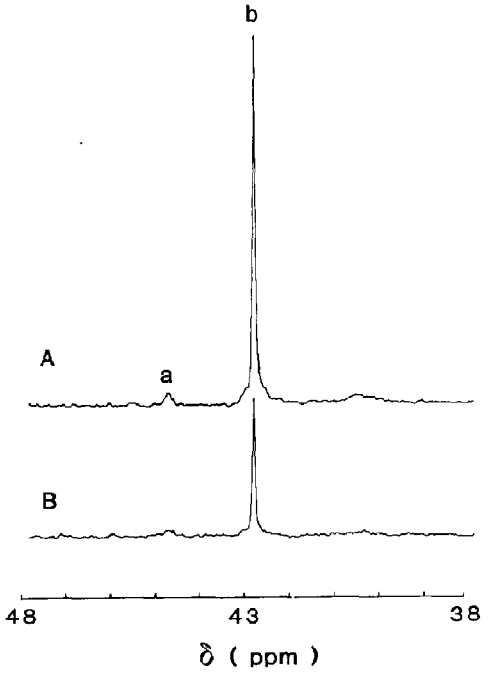

Fig. 6. Measurement of NOE of predominantly intracellular [α-^{13}C]glycine (b) in human erythrocytes in isotonic Krebs buffer; *Hc*, 0.80. NMR: 16 transients per spectrum; 37°C. Selective proton decoupling at resonance b. Spectrum A with NOE, spectrum B without NOE. Peak a is intracellular [*glycyl*-α-^{13}C]GSH.

Table 4

^{13}C-NMR T_1, NOE values and hydrodynamic parameters for [α-^{13}C]glycine and of [*glycyl*-α-^{13}C]GSH in erythrocytes at three representative cell volumes in two experiments (A, B) at 37°C

The final *Hc* of each suspension was 0.95. D_T was calculated from η_N-average using eq. 19, with Stokes radii: glycine, $r_o = (1.740 \pm 0.008) \times 10^{-8}$ cm; GSH, $r_o = (3.06 \pm 0.09) \times 10^{-8}$ cm. Uncertainty estimates represent 1 S.D.

		Cell volume (fl)		
		115.8	80.7	61.6
ECF π [a] (mosmol/kg)		215	300	577
ECF η_B [b] (mPa s)		0.756 ± 0.004	0.760 ± 0.003	0.769 ± 0.002
Glycine				
T_1 (s)	A	3.55 ± 0.18	3.45 ± 0.15	2.77 ± 0.18
	B	3.89 ± 0.07	2.97 ± 0.12	2.54 ± 0.12
NOE	A	3.00	–	–
	B	2.71	3.00	–
τ_r (s)($\times 10^{12}$)	A	6.56	6.75	8.41
	B	5.97	7.84	9.17
η_N (mPa s)	A	1.27 ± 0.07	1.31 ± 0.06	1.63 ± 0.11
	B	1.16 ± 0.03	1.52 ± 0.06	1.77 ± 0.09
η_N-average [c] (mPa s)		1.177 ± 0.028	1.42 ± 0.04	1.71 ± 0.07
D_t (cm^2/s)($\times 10^5$)		1.11 ± 0.03	0.92 ± 0.03	0.76 ± 0.03
GSH-glycyl				
T_1(s)	A		0.92 ± 0.08	
	B		0.84 ± 0.12	
τ_r (s)($\times 10^{12}$)	A		25.4	
	B		27.8	
η_N (mPa s)	A		0.91 ± 0.11	
	B		0.99 ± 0.17	
η_N-average [c] (mPa s)			0.934 ± 0.009	
D_T (cm^2/s)($\times 10^5$)			0.79 ± 0.02	

[a] Extracellular osmotic pressure.
[b] Extracellular fluid bulk viscosity.
[c] Weighted average of η_N A and B.

Table 5

Concentration-dependent interaction parameters [a] calculated for normalised bulk- and NMR-glycine-viscosity estimates of hemoglobin (Hb) in free solution and in human erythrocytes at 37°C

Hemoglobin solution					
[Hb] [b] (g/ml)		ϕ_{Hb} [c]	η_B (mPa s)	ν_B	κ_B
0.12		0.091	1.4 [d]	3.8 ± 0.5	2.27 ± 0.23
0.21		0.158	2.588 [d]		
0.315		0.238	7.388 [d]		
0.318		0.24	7.311		
Erythrocyte hemoglobin (probe: [α-^{13}C]glycine)					
Cell volume (fl)	[Hb] (g/ml)	ϕ_{Hb} [c]	η_N [e]	η_B [f]	ν_N	κ_N
115.8	0.241	0.182	1.537	2.47	2.480 ± 0.018	−0.253 ± 0.025
80.7	0.352	0.265	1.854	9.89		
61.6	0.468	0.353	2.232	632.36		

[a] All values of η were normalised to isotonic saline/^2H_2O (= 0.76 mPa s).
[b] Intracellular [Hb] calculated using eq. 22 for V_{ISO} = 80.7 fl.
[c] ϕ_{Hb} calculated using $\bar{v}$ = 0.7546 ml/g [21].
[d] η_B values from ref. 39.
[e] η_N values from table 5.
[f] Intracellular η_B values were predicted using eqs. 7 and 8.

Table 6

Literature estimates of intracellular viscosity in normal human erythrocytes at isotonicity

MCHC: mean corpuscular hemoglobin concentration. Uncertainty estimates represent ±1 S.D.

Method Probe	(Calibration)	Temperature (°C)	Viscosity (mPa s)	Ref.
(I) Viscometry				
1. Cell suspensions [a]		37	2–100	4
2. Hb solutions		37	7.4	39
(II) Predicted				
1. From MCHC		37	9–54	48, 65
(III) ESR				
1. Tempamine	(-)	18	4.19±0.07 [b]	6
2. Tempamine	(-)	25	4.9±1.8 [b]	7
3. Tempamine	(-)	21	3.3 [b]	8
4. MAL-5-GSH	(sucrose)	20	4.45±0.16	9
5. MAL-5-GSH	(sucrose)	37	2.5	9
(IV) NMR				
1. [α-^{13}C]Glycine	(BSA, Hb, glycerol)	37	1.38±0.03	3
2. [*glycyl*-α-^{13}C]GSH	(-)	37	1.26±0.11	3

[a] Absolute viscosity dependent on shear rate, hematocrit and MCHC.

[b] Calculated from relative viscosities by multiplying these by the absolute viscosity of pure water at the temperature indicated.

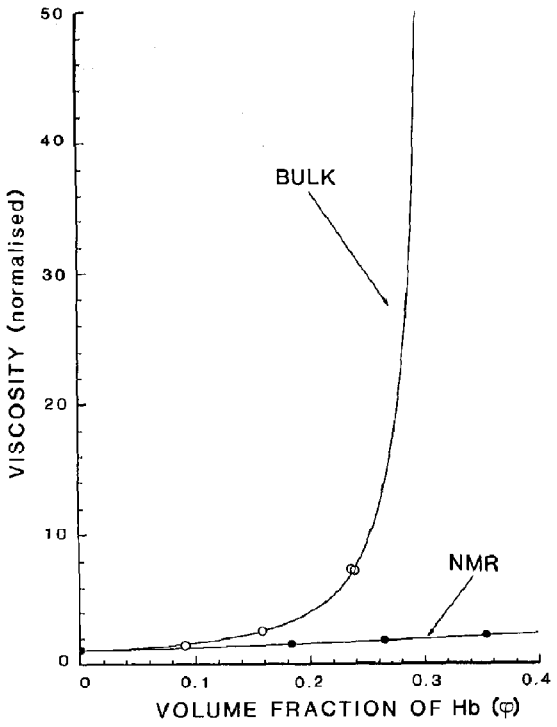

Fig. 7. Viscosity of Hb solutions at 37°C: (○) free solution (measured by Ostwald viscometry); (●) intracellular Hb (probed by [α-^{13}C]glycine). The intracellular Hb concentration was varied by changing the cell volume. The solid lines represent eq. 4 (cf. fig. 1) plotted using the interaction parameters listed in table 6. Viscosity measurements were normalised so that at $\phi = 0$, $\eta = 1$ (see footnote, table 5).

relationship between η_N and η_B in Hb solutions was qualitatively similar to that observed in BSA solutions. In particular, the theoretically expected values of η_B show an exponential increase as cell volume is reduced below normal, but this relative increase was not evident in the increase in the NMR-glycine-viscosity.

4.4. *Erythrocyte volume as a function of NMR-glycine-viscosity*

The theoretical relationship between erythrocyte volume and NMR-glycine-viscosity predicted by eq. 21 is shown in fig. 8; this was drawn using the hydrodynamic interaction parameters, ν_N and κ_N, given in table 5. Also shown are three esti-

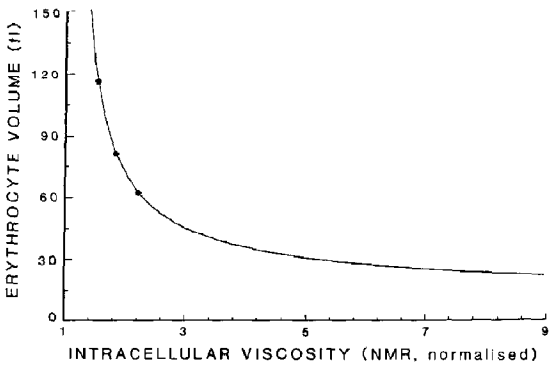

Fig. 8. Erythrocyte volume as a function of NMR-glycine-viscosity at 37°C. The solid line represents eq. 20, drawn using the viscosity interaction parameters calculated in table 5. The three points shown are the erythrocyte volume–(normalised) η_N data for glycine from table 4.

mates of η_N made at three different cell volumes (table 4). These points must fall on the theoretical line since they have been used to calibrate the NMR-glycine-viscosities as a function of ϕ_{HB}. However, once the NMR-probe-viscosity has been calibrated, a single measurement of T_1 of the intracellular-probe will allow calculation of the cell volume. It can also be seen that, with increasing NMR viscosity, the cell volume approaches asymptotically the volume occupied by the Hb molecules. However, since the erythrocyte membrane is not stable at cell volumes above approx. 140 fl, or below approx. 60 fl, the physiological range of normalised NMR-glycine-viscosities is from approx. 1.4 to approx. 2.2, i.e., an absolute viscosity range from approx. 1.1 to 1.7 mPa s; standard deviations of the volume estimates are approx. 10%.

5. Discussion

5.1. BSA and glycerol solutions

The use of ^{13}C-NMR and of ^{13}C-enriched glycine as a viscosity probe enables simple analysis of T_1 relaxation data: the low concentration of probe molecules and the finding of almost maximal NOE values indicated that the mechanisms contributing to this relaxation are purely dipole-dipole and intramolecular. Thus, the calculated correlation times represent purely rotational motion of the probe molecules that results ultimately from the Brownian motion of the solvent molecules.

The rate of rotational motion of a spherical probe in an ideal solution is given by eq. 9 (but including the microfrictional coefficient). Therefore, at low solute concentrations, the viscosities obtained from τ_r values by using eqs. 16 and 17, viz., NMR-probe-viscosities, should equal the bulk viscosity of the solution. This equality was observed at low solute concentrations in both BSA and glycerol solutions (figs. 1 and 2)

The calculation of the Stokes radius, r_0, from τ_r in the solution of lowest bulk viscosity empirically takes account of the coefficient of microfriction, ξ. It is therefore possible to estimate ξ for spherical (or ellipsoidal) rotors by comparing NMR viscosity values calculated using eq. 16 (or 17) and experimental geometrical factors with values of η_N calculated using r_o determined directly from the molecular geometry. For example, in isotonic saline (bulk viscosity = NMR viscosity = 0.76 mPa s; tables 1 and 2) at 37°C the measured τ_r(glycine) was 3.8856×10^{-11} s which gives an empirical value of r_0 of 1.74 Å. The dimensions of the zwitterionic glycine molecule were estimated from a CPK model (Corey-Pauling-Koltun; Ealing, Waterford, U.K.) by using Vernier callipers. This gave 3.06, 2.28 and 2.08 Å respectively for the x, y and z axes of an ellipsoid; a symmetrical prolate ellipsoid of equal volume would have semiaxes major (a) and minor (b) lengths of 3.06 and 2.27 Å, respectively, and an equivalent volume sphere would have a radius = $(ab^2)^{1/3}$ = 2.51 Å. At the same value of τ_r, application of eq. 16 to the sphere with radius 2.51 Å would give a value of 0.25 mPa s for the NMR viscosity. Therefore, ξ = [NMR viscosity (known dimension)]/[NMR viscosity (empirical dimension)] = 0.5/0.76 = 0.33. This compares well with the theoretical estimate for glycine in water, which was calculated to be 0.23 by using eq. 10 and a Van der Waals radius of water of 1.6 Å [22].

Since eq. 9 was derived for ideal solutions [24,32,33] it was not surprising that in con-

centrated BSA and glycerol solutions substantial deviation occurred between the bulk and NMR viscosity values. It was possible to quantify this deviation by applying theory developed for concentrated suspensions of spheres (eq. 4) to both NMR and bulk viscosity estimates obtained for the same solutions. This allowed two sets of phenomenological hydrodynamic interaction parameters (ν_N, κ_N) and (ν_B, κ_B) to be obtained for each probe-solute-solvent system. These were then used to calculate the bulk viscosity from the NMR viscosity and vice versa by applying eqs. 5–8. Similarly, by using eq. 20, we calculated the concentration-dependent deviation of probe τ_r values from those predicted for an ideal solution (by eq. 9).

It was also observed that different τ_r and NMR viscosity values were obtained when using the same concentration of [α-^{13}C]glycine probe molecules in BSA and glycerol solutions having identical bulk viscosities (fig. 3). Furthermore, in the case of glycerol solutions, the use of a self-probe yielded values different from those obtained with [α-^{13}C]glycine (fig. 2). These results indicate that estimates of NMR viscosity are unique to each probe-solute-solvent system and will yield unique values in different systems even if the bulk viscosities of the systems are the same. Consequently, it is incorrect to infer a 'microviscosity' of a sample from a particular value of τ_r using probe τ_r values that have been calibrated against bulk viscosity in a solution of substantially different composition. Such considerations apply to ESR estimates of erythrocyte microviscosity obtained following calibration of the spin-probes in either glycerol or sucrose solutions [7,9,40]. Indeed, the term microviscosity is best avoided unless the probe molecule is also specified; as in 'glycine microviscosity'. We have avoided this term altogether and have specified both the method and probe molecule, as in 'NMR-glycine-viscosity'.

Both long- and short-range interactions may occur between probe and other solute molecules. However, it is unlikely that significant differences in electrostatic interaction were present in BSA compared with glycerol solutions since within the experimental pH range in both solutions glycine was zwitterionic (the pK_a values of glycine are 2.35 and 9.78; [41]), and the experiments were conducted in a polar solvent containing abundant NaCl (50–154 mmol/l). In any case any interaction model must account for the similar exponential concentration dependence of glycine and glycerol τ_r values in glycerol solutions; this is in contrast to the almost linear concentration dependence of glycine τ_r values in BSA and Hb solutions.

A simple geometric model is therefore proposed to account for the different degrees of interaction between the probe and solute in the different solutions. The model assumes that the molecular interaction between probe and solute molecules is purely hydrodynamic; the interactions which produce the changes in τ_r and NMR viscosity vary with the relative sizes of the probe and solute molecules. Where the solute is much larger, e.g., a glycine probe in BSA solution, the solute will have little hydrodynamic influence on the free rotation of the probe. Where they are of similar size, e.g., a glycine probe in glycerol solution, small changes in solute concentration will readily alter probe rotation rates. Such differences may be a manifestation of a greater degree of shielding of the probe by solvent where the probe-solute size difference is large. For instance, if BSA molecules (assumed to be spheres) are completely 'close-packed' in a hexagonal lattice, large gaps comprising 26% of the available volume will remain in which the small probe molecules, shielded by water, can undergo relatively unrestricted rotational and, to a lesser extent, translational diffusion. Thus despite an exponential increase in the bulk viscosity as $\phi \rightarrow 0.74$ there will be only a small increase in τ_r(glycine) and hence the NMR-glycine-viscosity. Consistent with this model is the finding that, when intracellular viscosity is increased by allowing human erythrocytes to equilibrate with glycerol (to a calculated intracellular glycerol concentration of 30 g/dl), the τ_r and NMR-glycine-viscosity values reflect only the glycerol concentration so that the normal intracellular-extracellular viscosity difference is eliminated [42]. This has been suggested as a possible basis for the cryprotective effect of glycerol during storage of human erythrocytes [42].

5.2. Intact human erythrocytes

The finding of a value of approx. 1.4 mPa s for NMR-glycine-viscosity in intact normovolemic cells at 37°C (table 4, cell volume 80.7 fl) confirms previous observations [3] and also confirms that NMR viscosity estimates are significantly smaller in magnitude than those obtained by other methods (table 5). There are several possible reasons for higher values of intracellular probe viscosities determined by ESR. First, the probes used in ESR measurements are larger than glycine and, as indicated by the results reported for BSA and glycerol solutions, a larger probe molecule will give larger values of τ_r and viscosity. Secondly, some ESR probes partition into the cell membrane, e.g., Tempone [6,10,43] and possibly also Tempamine [7,9]. Thirdly, ESR probe correlation times were not calibrated in Hb solutions, but rather in glycerol and sucrose solutions [7,9,40]

The observed changes in intraerythrocyte NMR-glycine-viscosity with alteration of cell volume follow the expected change in the concentration of Hb; as cell volume decreased from 115.8 to 61.6 fl the average NMR-glycine-viscosity increased from approx. 1.2 to approx. 1.7 mPa s (table 4). While a qualitative change of this type is easy to anticipate, its occurrence has only recently been verified directly by using ESR; however, as indicated above, ESR probe viscosity estimates yield a higher viscosity range depending on the specific probe and temperature used; approx. 3 to approx. 8 mPa s for 2,2′,5,5′-tetramethyl-3-maleimidopyrrolidinyl-*N*-oxyl-GSH (MAL-5-GSH) at 20°C [9] and approx. 1.56 to approx. 5 mPa s for Tempamine at 25°C [7]. These three different viscosity ranges support the hypothesis advanced above that τ_r measurements in concentrated solutions give estimates of viscosity which vary directly with the relative size of the probe molecule (in the absence of internal or segmental motion within the probe).

It is therefore suggested that the correct viscosity estimate is the one which defines the restriction of motion pertinent to the system under investigation. This is illustrated by two examples:

5.2.1. Diffusion-controlled enzymic reactions

In order to ascertain whether a particular reaction is subject to diffusion control, the coefficients for translational diffusion (D_T) of the reactants in the reaction medium are required in order to calculate the theoretical second-order rate constants (k_1 for a bimolecular reaction [44]). The calculated value of k_1 may then be compared with experimental values. Alternatively, the collision frequency between substrate and enzyme may be estimated directly from the viscosity of the reaction medium [45]. However, while the self-diffusion of proteins in aqueous solutions is approximately inversely proportional to the solution viscosity, this is not the case for small molecules such as water in protein solution [46]. Furthermore, it is difficult in intact cells to use traditional means of measuring diffusion coefficients, since diffusion is restricted. On the other hand, it is relatively simple to use eq. 19 to calculate D_T from the viscosity actually experienced by the molecule in situ, i.e., from the NMR or ESR probe viscosity [3].

In the normal circulation, erythrocytes traverse osmolalities ranging from 287 mosmol/kg in the general circulation [47] to 1200 mosmol/kg in the vasa recta at the tip of the renal medulla [48]. Consequently, human erythrocytes may undergo almost the entire range of volume changes depicted in fig. 8. Consequently, such volume changes should (transiently) alter the rate of diffusion-controlled reactions involving small substrates similar in size to glycine to the same extent that NMR-glycine-viscosity is altered, i.e., by a factor of approx. $1.7/1.2 = 1.4$. An example of such a reaction is that catalysed by superoxide dismutase, which has a second-order k_1 of 2×10^9 l/mol per s [49,50]. Greater changes in reaction rate may occur if the substrates are larger or are normally present in 'limiting' concentration, i.e., much below the Michaelis constant of the enzyme involved.

5.2.2. Cell deformability

Reversible isochoric changes in erythrocyte shape occur continuously in vivo in the dynamic circulation and are essential for cell survival during passage through normal capillaries 4–7 μm in

diameter and particularly during diapedesis where erythrocytes passing through splenic sinusoids must traverse interendothelial slits 0.2–0.5 μm wide [51,52]. Since deformation involves bending and local stretching of the membrane as well as the flow of the internal fluid, cell deformability is a function of the flexibility of the membrane and the viscosity of the cytoplasm [53,54]. Since the contribution of the intracellular viscosity to deformability involves flow, the appropriate measure is the bulk viscosity, which can be calculated from the NMR-probe-viscosity using eqs. 7 and 8. As shown in fig. 8, a halving of erythrocyte volume (from approx. 120 fl) will produce an exponential increase in the bulk viscosity of the cytoplasm (to approx. 484 mPa s). An exponential increase in the bulk viscosity may be anticipated with the onset of close packing of the intracellular protein molecules. The edge-to-edge separation between Hb spheres was estimated, using eq. 33, to be 32, 22 and 15 Å at cell volumes of 115.8, 80.7 and 61.6 fl, respectively. These distances confirm that the intracellular bulk viscosity increased exponentially when the intermolecular separation of Hb molecules was less than the molecular radius of Hb ($\sim$ 27 Å), i.e., with the onset of close packing. As anticipated from the experiments in BSA solutions, the intracellular NMR-glycine-viscosity increased only slowly over the same cell volume range. This disparity between intracellular bulk- and NMR-viscosity estimates is corroborated by the finding that Tempone correlation times in gelled solutions of deoxyhemoglobin S are no greater than those in non-gelled Hb of the same total concentration [55] (table 6).

Small increases in intracellular bulk viscosity may be of physiological significance. Erythrocyte aging is associated with an increase in density and a corresponding increase in the mean corpuscular Hb concentration from 0.317 to 0.375 g/ml [56,57]. These values indicate that the bulk viscosity changes from approx. 5.6 to approx. 15.3 mPa s while the NMR-glycine-viscosity increases from approx. 1.3 to approx. 1.5 mPa s. It has been suggested that cellular rigidity may determine the survival of erythrocytes in the circulation [58]. By reducing erythrocyte deformability and delaying the passage of erythrocytes through the spleen, the calculated 3-fold increase in bulk viscosity could well determine the clearing of senescent cells from the circulation. However, it seems unlikely that the small associated increase in the viscosity experienced by small molecules (illustrated by the increase in the NMR-glycine-viscosity) could explain the decrease in enzymic activity in old erythrocytes reported for superoxide dismutase [59].

Finally, the use of eq. 21 to calculate the cell volume from the intracellular NMR-glycine-viscosity (fig. 8) illustrates that, after calibration, a single measurement of the intracellular glycine T_1 will allow erythrocyte volume to be determined as well as the intracellular viscosity; although a more precise NMR method for the former parameter has recently been reported [66].

Appendix A: Interrelationship between bulk and NMR viscosity

Rewriting eq. 5 by using the subscript B to denote bulk viscosity and making ϕ the subject, gives:

$$\phi_B = \ln(\eta_B)/[\nu_B + \kappa_B \ln(\eta_B)]. \quad \text{(A1)}$$

An identical expression may be written in terms of ϕ_N with the subscript N denoting the NMR-probe-viscosity:

$$\phi_N = \ln(\eta_N)/[\nu_N + \kappa_N \ln(\eta_N)]. \quad \text{(A2)}$$

Since bulk and NMR viscosity measurements were obtained for the same solutions $\phi_B = \phi_N = \phi$. Combining eqs. A1 and A2 gives:

$$\eta_N = \eta_B^{\psi}, \quad \text{(A3)}$$

where

$$\psi = \nu_N/\{\nu_B + \ln(\eta_B)[\kappa_B - \kappa_N]\}. \quad \text{(A4)}$$

By a similar procedure an expression for η_B is found. This is of identical form to η_N but with the subscripts interchanged and is given in section 2 (eqs. 7 and 8).

Since τ_r is determined ultimately by the forces acting in the local environment of the molecular species it is appropriate to define it according to

the local viscosity, i.e., the NMR viscosity; accordingly eq. 16 becomes,

$$\tau_r = (4\pi r_o^3/3kT)\eta_N. \quad \text{(A5)}$$

Appendix B: Cell volume as a function of intraerythrocyte NMR viscosity

Substituting $c\bar{v}$ for ϕ in eq. A2 gives:

$$c = \{\bar{v}[\nu_N/\ln(\eta_N) + \kappa_N]\}^{-1}. \quad \text{(B1)}$$

Hb is the principal space-occupying solute in erythrocytes; therefore c = mass(Hb)/(intracellular volume). The mass of Hb in a cell is constant and given by:

$$\text{mass(Hb)} = Hb_{ISO}V_{ISO}(1 - F), \quad \text{(B2)}$$

where Hb_{ISO}, V_{ISO} and F are defined in section 3. Consequently, the intracellular solution volume, V_{IC}, is given by:

$$V_{IC} = Hb_{ISO}V_{ISO}(1 - F)\{\bar{v}[\nu_N/\ln(\eta_N) + \kappa_N]\}. \quad \text{(B3)}$$

The total erythrocyte volume V is equal to $(V_{IC} + FV_{ISO})$ so that,

$$V = V_{ISO}\{F + \bar{v}Hb_{ISO}(1 - F)[\nu_N/\ln(\eta_N) + \kappa_N]\}. \quad \text{(B4)}$$

Note that it is also possible to rewrite eq. B4 as a function of the extracellular osmolality using a published expression for erythrocyte osmometer behaviour [14].

Appendix C: Intermolecular separation of Hb molecules in erythrocyte cytoplasm

Hb molecules are assumed to be spherical, non-aggregated, and maximally and symmetrically dispersed in the cytoplasm. When the Hb concentration is maximal, the Hb spheres will be arranged in cubic closest packing. Hence each sphere will have a coordination number of 12 [60]. If the space remaining between such maximally close-packed spheres is equally divided among the spheres, each sphere will be enclosed in a regular rhombic dodecahedron and touch each adjacent sphere at the midpoint of the rhombic face [60]. Thus, the Hb molecule can be considered as the insphere of a regular rhombic dodecahedron, i.e., the radius of Hb (R_{Hb}) equals the radius of the insphere (R_I). When the Hb concentration is submaximal, the centre of the Hb spheres is assumed to remain at the centre of the rhombic dodecahedron, but now $R_{Hb} < R_I$. The edge-to-edge separation between Hb molecules is then given by $2(R_I - R_{Hb})$.

If the shorter diagonal of each rhombic face has length $2L$, then the radius of the insphere (R_I) is $L/2$ and the centre-to-centre distance between adjacent spheres is $2L\sqrt{2}$. N such dodecahedra will have a volume of $16NL^3$; therefore, for unit volume of solution $L = (1/16N)^{1/3}$. Since N represents the number of Hb spheres enclosed by rhombic dodecahedra, then in one cell,

$$L = [M/16cN_A]^{1/3} \quad \text{(C1)}$$

since cN_A/M is the number of Hb molecules per cell; c is the concentration (g/ml), M the molecular weight and N_A Avogradro's number. The radius of the insphere is therefore given by:

$$R_I = \sqrt{2}[M/16cN_A]^{1/3} \quad \text{(C2)}$$

Since the volume of one Hb molecule is equal to $M\bar{v}/N_A$, where $\bar{v}$ is the measured partial specific volume (ml/g), then the radius of Hb is given by

$$R_{Hb} = [3M\bar{v}/4\pi N_A]^{1/3} \quad \text{(C3)}$$

Thus, the intermolecular separation (in dm) is given by:

$$\text{Separation} = 2[M/N_A]^{1/3}\{[1/2c]^{1/3}/\sqrt{2} - [3\bar{v}/4\pi]^{1/3}\}. \quad \text{(C4)}$$

Since the volume fraction, ϕ, $= c\bar{v}$, then eq. C4 may be written as:

$$\text{Separation} = 2[\bar{v}M/N_A]^{1/3}\{[1/4\phi\sqrt{2}]^{1/3} - [3/4\pi]^{1/3}\} \quad \text{(C5)}$$

An important result from eq. C5 is that the intermolecular separation is zero when ϕ =

$\pi/3\sqrt{2} = 0.74048.....$; thus, provided that 12 is the maximum coordination number, then 0.74 is the maximum packing density of close packed spheres.

In order to apply this method generally to the calculation of intersphere distances, all that is required is an estimate of N, the number of spheres per unit volume and the absolute value of the sphere radius. For example, the separation between erythrocytes in suspension can be calculated from the hematocrit (Hc) if the cells are assumed to be spherical. N, the number of cells (per mm^3) is given by:

$$N = (Hc/V) \times 10^3 \qquad \text{(C6)}$$

where V is the cell volume (fl) and Hc is fractional [61]. Assuming V to be constant and normal, e.g., 90 fl, then eq. C2 becomes:

$$R_I = \sqrt{2}\left[90/(Hc \times 16 \times 10^{12})\right]^{1/3} \qquad \text{(C7)}$$

with R_I given in cm. A sphere of volume 90 fl has a radius of 2.78×10^{-4} cm. An equation for intercellular separation (cm) analogous to eqs. C4 and C5 is therefore:

$$\text{Separation} = 2\left\{\left[1.591 \times 10^{-11}/Hc\right]^{1/3} - 2.78 \times 10^{-4}\right\}. \qquad \text{(C8)}$$

Eq. C8 simplifies further to:

$$\text{Separation} = \left[5.032/(Hc)^{1/3} - 5.56\right] \times 10^{-4}. \qquad \text{(C9)}$$

Using the radius of the sphere (2.78×10^{-4} in this example) as a distance parameter, estimates of intercellular separation obtained using eq. C9 may also be expressed in terms of radii using:

$$\text{Separation}' = \text{Separation}/(2.78 \times 10^{-4}). \qquad \text{(C10)}$$

Adding 2 to the result of eq. C10 yields the centre-to-centre separation between the spheres. It should be noted that eqs. C8 and C9 both yield a value of zero when $Hc = 0.74$.

Acknowledgements

The work was supported by a post graduate scholarship to Z.H.E. and a project grant to P.W.K., from the Australian National Health and Medical Research Council. The assistance of Mr. Brian Bulliman and Dr. B.E. Chapman with computing and in the use of the NMR spectrometer, respectively, is gratefully acknowledged.

References

1 R.C. Weast, Handbook of chemistry and physics (CRC Press, Cleveland, OH, 1975).
2 R. Glaser, H. Heinrich, M. Brumen and S. Svetina, Biomed. Biochim. Acta 42 (1983) S77.
3 Z.H. Endre, B.E. Chapman and P.W. Kuchel, Biochem. J. 216 (1983) 655.
4 L. Dintenfass, Haematologia. 2 (1968) 19.
5 S. Chien, in: The red blood cell, ed. D.M. Surgenor, 2nd edn. (Academic Press, New York, 1975) vol. II, p. 1031.
6 P.D. Morse, Biochem. Biophys. Res. Commun. 77 (1977) 1486.
7 P.D. Morse, D.M. Lusczakoski and D.A. Simpson, Biochemistry 18 (1979) 5021.
8 G. Bartosz and W. Leyko, Blut 41 (1980) 131.
9 D. Daveloose, G. Fabre, F. Berleur, G. Testylier and F. Leterrier, Biochim. Biophys. Acta 763 (1983) 41.
10 A.D. Keith and W. Snipes, Science 183 (1974) 666.
11 R. Cooke and I.D. Kuntz, Annu. Rev. Biophys. Bioeng. 3 (1974) 95.
12 F. Franks and S. Mathias, Biophysics of water (John Wiley, Chichester, 1982).
13 M.J. York, P.W. Kuchel and B.E. Chapman and A.J. Jones, Biochem. J. 207 (1982) 65.
14 Z.H. Endre, P.W. Kuchel and B.E. Chapman, Biochim. Biophys. Acta 803 (1984) 137.
15 G. Robinson, P.W. Kuchel, B.E. Chapman, D.M. Doddrell and M.G. Irving, J. Mag. Reson. 63 (1985) 314.
16 D.E. Woessner, J. Chem. Phys. 37 (1962) 647.
17 D. Doddrell, V. Glushko and A. Allerhand, J. Chem. Phys. 56 (1972) 3683.
18 M. Mooney, J. Colloid Sci. 6 (1951) 162.
19 A. Einstein, Ann. Phys. 19 (1906) 289.
20 A. Einstein, Ann. Phys. 34 (1911) 591.
21 J. Bernhardt and H. Pauly, J. Phys. Chem. 79 (1975) 584.
22 F.M. Richards, Annu. Rev. Biophys. Bioeng. 6 (1977) 151.
23 C. Chothia, Nature 254 (1975) 304.
24 N. Bloembergen, E.M. Purcell and R.V. Pound, Phys. Rev. 73 (1948) 679.
25 A. Gierer and K. Wirtz, Z. Naturforsch. 8a (1953) 532.
26 J.H. Noggle and R.E. Schirmer, The nuclear Overhauser effect. Chemical applications (Academic Press, New York, 1971) p. 4.
27 H.L. Frisch and R. Simha, in: Rheology, ed. F.R. Eirich (Academic Press, New York, 1956) vol. 1, p. 525.
28 R.E. London, C.E. Hildebrand, E.S. Olson and N.A. Matwiyoff, Biochemistry 15 (1976) 5480.
29 G.G. Stokes, Trans. Camb. Phil. Soc. 8 (1849) 287.

30 G.G. Stokes, Trans. Camb. Phil. Soc. 9 (1856) 8.
31 A. Einstein, Ann. Phys. 19 (1906) 371.
32 P. Debye, Ber. Dtsch. Phys. Ges. 15 (1913) 777.
33 P. Debye, Polar molecules (Dover, New York, 1927) ch. 5.
34 R.B. Pennell, in: The red blood cell, ed. D.M. Surgenor, 2nd edn. (Academic Press, New York, 1974) vol. II, p. 93.
35 E. Beutler, Red blood cell metabolism: a manual of biochemical methods, 2nd edn. (Grune & Stratton, New York, 1975) p. 13, 149.
36 J.E. McKie and J.F. Brandts, Methods Enzymol. 26 (1972) 257
37 M.R. Osborne, J. Aust. Math. Soc. B. 19 (1976) 343.
38 M. Kendall and A. Stuart, The advanced theory of statistics (Charles Griffin, London, 1977) vol. I, ch. 10.
39 G.R. Cokelet and H.J. Meiselman, Science 162 (1968) 275.
40 S.P. Berg, D.M. Luseczakoski and P.D. Morse, Arch. Biochem. Biophys. 194 (1979) 138.
41 G.H. Aylward and T.J.V. Findlay, SI chemical data (John Wiley & Sons, Milton, Qld, 1974).
42 Z.H. Endre, B.E. Chapman and P.W. Kuchel, Biomed. Biochim. Acta. 3 (1984) S83.
43 E.D. Finch and J.F. Harmon, Science 186 (1974) 157.
44 R.A. Alberty and G.G. Hammes, J. Phys. Chem. 62 (1958) 154.
45 A.D. Keith, E.C. Pollard, W. Snipes, S.A. Henry and M.R. Culbertson, Biophys. J. 17 (1977) 205.
46 J.H. Wang, J. Am. Chem. Soc. 76 (1954) 4755.
47 G.L. Robertson, R.L. Shelton and S. Athar, Kidney Int. 10 (1976) 25.
48 C.W. Gottschalk and M. Mylle, Am. J. Physiol. 196 (1959) 927.
49 G. Rotilio, R.C. Gray and E.M. Fielden, Biochim. Biophys. Acta 268 (1972) 605.
50 B.G. Malmström, L.-E. Andreasson and B. Reinhammer, in: The enzymes, ed. P.D. Boyer (Academic Press, New York, 1975) p. 533.
51 A.J. Grimes, Human red cell metabolism (Blackwell, Oxford, 1980) p. 93, 192, 281.
52 R.S. Weinstein, in: The red blood cell, ed. D.M. Surgenor, 2nd edn. (Academic Press, New York, 1975) vol. I, p. 213.
53 L. Dintenfass, Angiology 13 (1962) 333.
54 L. Dintenfass, Acta Haematol. 32 (1964) 299.
55 A.G. Beaudoin and H. Mizukami, Biochem. Biophys. Acta 532 (1978) 41.
56 S. Piomelli, G. Lurinsky and L.R. Wasserman, J. Lab. Clin. Med. 69 (1967) 659.
57 S. Usami, S. Chien and M.I. Gregersen, in: Haemorheology, ed. A.L. Copley (Pergamon Press, Oxford, 1971) p. 266.
58 A.R. Williams and D.R. Morris, Scand. J. Haematol. 24 (1980) 57.
59 G. Bartosz, C. Tannert, R. Fried and W. Leyko, Experientia 34 (1978) 1464.
60 H.S.M. Coxeter, Introduction to geometry (Wiley, New York, 1969) p. 396.
61 J.V. Dacie and S.M. Lewis, Practical haematology, 5th edn. (Churchill Livingstone, Edinburgh, 1975) ch. 2.
62 R. Roscoe, Br. J. Appl. Phys. 3 (1952) 267.
63 H.C. Brinkman, J. Chem. Phys. 20 (1952) 571.
64 R. Simha, J. Appl. Phys. 23 (1952) 1020.
65 A.J. Erslev and J. Atwater, J. Lab. Clin. Med. 62 (1963) 401.
66 K. Kirk and P.W. Kuchel, J. Magn. Reson. 62 (1985) 568.